# NACA

# RESEARCH MEMORANDUM

HINGE-MOMENT CHARACTERISTICS FOR A SERIES OF CONTROLS

AND BALANCING DEVICES ON A 60° DELTA WING AT

MACH NUMBERS OF 1.61 AND 2.01

By Douglas R. Lord and K. R. Czarnecki

Langley Aeronautical Laboratory Langley Field, Va.

# NATIONAL ADVISORY COMMITTEE FOR AERONAUTICS

WASHINGTON

April 12, 1957 Declassified May 29, 1959

# NATIONAL ADVISORY COMMITTEE FOR AERONAUTICS

#### RESEARCH MEMORANDUM

HINGE-MOMENT CHARACTERISTICS FOR A SERIES OF CONTROLS

AND BALANCING DEVICES ON A 60° DELTA WING AT

MACH NUMBERS OF 1.61 AND 2.01

By Douglas R. Lord and K. R. Czarnecki

#### SUMMARY

An investigation has been made to determine the control hinge-moment characteristics at Mach numbers of 1.61 and 2.01 for a series of 18 controls, including the effects of various tabs and fences, on a  $60^{\circ}$  delta wing. Tests were made at a Reynolds number of  $4.2 \times 10^{\circ}$  (based on the mean aerodynamic chord of the wing) and covered ranges of angles of attack from  $0^{\circ}$  to  $12^{\circ}$ , control deflection from  $-30^{\circ}$  to  $30^{\circ}$ , and tab deflection from  $0^{\circ}$  to  $-20^{\circ}$ .

The hinge-moment-slope parameters for the basic tip controls correlated satisfactorily with the ratio of balance-control area to total-control area at a Mach number of 2.01. The experimental hinge-moment-slope parameters for the trailing-edge controls were 70 percent as large as those of the theoretical predictions. Increasing the trailing-edge thickness on a trailing-edge control increased the hinge-moment-curve slopes. A parting-line fence forward of the hinge line on a closely balanced tip control resulted in improved hinge-moment characteristics. A detached tab was more effective than an inset or attached tab on a tip control in balancing the hinge moments due to control deflection. An attached tab on a full-span trailing-edge control had more balancing effect when located outboard than when located inboard. Paddle balances on a full-span trailing-edge control decreased the slope of the hinge-moment-coefficient variation with control deflection.

#### INTRODUCTION

As part of a general program of research on controls, an investigation is underway in the Langley 4- by 4-foot supersonic pressure tunnel to determine the important parameters in the design of controls for use on a 60° delta wing at supersonic speeds. The results have been obtained

from two series of tests by means of pressure distributions and direct measurements of the hinge moments. The first series was conducted at a Mach number of 1.61 and included primarily tip controls, some fence configurations, and a trailing-edge control with and without a spoiler mounted on the wing just ahead of the control. Many of the control hinge-moment and effectiveness results and some illustrative pressure distributions from this series have been presented in references 1 to 5. The second series included tests of several trailing-edge controls, two additional tip controls, and several tab and fence configurations, each at a Mach number of 1.61, and four of the tip controls at a Mach number of 2.01.

The purpose of this report is to present the hinge-moment data and analysis which have not previously been reported for the 18 configurations and to compare the results obtained with those already presented. The tests were made for a wing angle-of-attack range from 0° to 12°, for a control deflection range from -30° to 30°, and, where applicable, for a tab deflection range from 0° to -20°. All configurations were tested at a Reynolds number of 4.2 × 10° based on the wing mean aerodynamic chord of 12.10 inches.

#### SYMBOLS

Ch	hinge-moment coefficient of control (trailing-edge controls), H/q2Q
Ch,1	hinge-moment coefficient of control (tip controls), $H/qS\bar{c}$
ē	mean aerodynamic chord of control
Н	hinge moment of control
М	Mach number
Mt	tab area moment about control hinge line
Q	area moment of control surface behind hinge line about hinge line (excluding tab, where present)
q	stream dynamic pressure
S	plan-form area of control (excluding tab, where present)
$S_{B}$	plan-form area of control ahead of hinge line

- α wing angle of attack
- δ control deflection relative to wing (positive when control trailing edge is deflected down)
- δt tab deflection relative to control (positive when tab trailing edge is deflected down)
- △ prefix indicating increment due to tab or fence

# Subscripts:

- $\alpha$  slope of coefficient variation with  $\alpha$
- $\delta$  slope of coefficient variation with  $\delta$
- $\delta_{t}$  slope of coefficient variation with  $\delta_{t}$

(All slopes were taken at  $\alpha = 0^{\circ}$ ,  $\delta = 0^{\circ}$ ,  $\delta_{+} = 0^{\circ}$ .)

### APPARATUS

## Wind Tunnel

This investigation was conducted in the Langley 4- by 4-foot supersonic pressure tunnel which is a rectangular, closed-throat, single-return wind tunnel with provisions for the control of pressure, temperature, and humidity of the enclosed air. Flexible-nozzle walls were adjusted to give the desired test-section Mach numbers of 1.61 and 2.01. During the tests, the dewpoint was kept below -20° F; so that the effects of water condensation in the supersonic nozzle were negligible.

# Model and Model Mounting

The model used in this investigation consisted of a semispan delta wing with interchangeable controls and various associated control adapters (or replacement sections) that were required to fit the control to the basic wing component. The control configurations are presented in figure 1 and are grouped according to whether they are tip controls (fig. l(a)), tip controls with tabs or fences (fig. l(b)), or trailingedge controls (fig. l(c)).

The basic wing had a  $60^{\circ}$  sweptback leading edge, a root chord of 18.14 inches, and a semispan of 10.48 inches. The wing had a rounded

NACA 63-series section extending 30 percent of the root chord back from the leading edge, a constant-thickness center section with a thickness-chord ratio of 3 percent based on the root chord, and a sharp trailing edge. (See fig. 1(a).) Near the wing tip, the nose section joined directly to the tapered trailing edge without a flat midsection. Configurations J-1 and J-2 had thickened trailing edges as shown in the sketches of figure 1(c).

The basic wing and controls were constructed of steel. (For details of construction, see ref. 1.) The paddle balances of configuration J-3, the tab of configuration E-1, and the inset and detached tabs on configuration E were also constructed of steel. The tabs on configuration J and the fences were constructed of 1/16-inch stock brass.

The semispan wing was mounted horizontally on a turntable in a steel boundary-layer bypass plate which was located vertically in the test section approximately 10 inches from the sidewall, as shown in figures 2 and 3.

#### TESTS

The angle of attack of the model was changed by rotating the turntable in the bypass plate on which the wing was mounted (see fig. 2) and was measured by a vernier on the outside of the tunnel, inasmuch as the angular deflection of the wing under load was negligible. Controls were deflected by a gear mechanism, mounted on the pressure box, which rotated as a unit the strain-gage balance, the torque tube, and the control. The control deflections were set approximately with the aid of an electrical control-position indicator mounted on the torque tube near the wing-root and were measured under load during testing with a cathetometer mounted outside the tunnel.

Hinge moments of the controls were determined by means of an electrical strain-gage beam located in the pressure box (fig. 2), which measured the torque on the tube actuating the control surface. Interchangeable strain-gage beams with various load ranges were used to obtain greater accuracy for the closely balanced controls.

Tests were made over an angle-of-attack range from  $0^{\circ}$  to  $12^{\circ}$  at increments of either  $3^{\circ}$  or  $6^{\circ}$ . The control-deflection range was from  $-30^{\circ}$  to  $30^{\circ}$  at increments of  $5^{\circ}$ , and the tabs were tested at deflections of  $0^{\circ}$ ,  $-10^{\circ}$ , and  $-20^{\circ}$ . The tests were made at tunnel stagnation pressures of 15 and 17.5 pounds per square inch absolute and at Mach numbers of 1.61 and 2.01, respectively. The stagnation pressures and the Mach numbers correspond to a Reynolds number of  $4.2 \times 10^{\circ}$  based on the wing mean aerodynamic chord of 12.10 inches. Although no attempt was made to fix transition on the model, the surface roughness was probably great enough to cause a turbulent boundary layer.

#### PRECISION OF DATA

The mean Mach numbers in the region occupied by the model were estimated from calibration to be 1.61 and 2.01 with local variations smaller than ±0.02. There was no evidence of significant flow angularity. The estimated accuracy of other pertinent quantities is as follows:

α, deg											±0.05
δ, deg											±0.1
$\delta_t$ , deg	٠										±0.1
Ch (measured directly) .											±0.005
Ch.1 (measured directly)											±0.005

## RESULTS AND DISCUSSION

# Basic Variations of Hinge-Moment Coefficients

The basic hinge-moment-coefficient variations with control deflection are presented in figures 4 through 14 in the order that the configurations are shown in figure 1. In addition to the basic curves obtained from the strain-gage measurements, the curves determined by integration of the pressure distributions over the controls are shown for comparison. The description of the pressure-orifice installation and the tabulated pressure data can be obtained from reference 5. No integrated results are presented herein for the tab configurations or the paddle-balance configuration, because there were no orifices on the tabs or paddles and no integrated results are presented for configuration K, which had no orifices on the tip control.

In general, the hinge-moment curves obtained by integrating the surface pressures show the same trends as those obtained by the direct measurements. Sizable differences occur for many of the configurations, however, because of the lack of sufficient orifices to define more precisely the chordwise and spanwise distributions of loading. As was previously shown in reference 1, the more closely balanced tip controls exhibited regions of overbalance (for example, figs. 4(c) and 5(b)). At the largest angle of attack, many of the controls also produced very nonlinear variations of hinge-moment coefficient with control deflection. (For example, see figs. 4(c), 5(a), and 5(b).) The trailing-edge controls indicated a greater effect of viscosity as evidenced by the sharp decrease in slope of the hinge-moment curves at the largest control deflections. (For example, see figs. 10, 13(a), and 13(b).)

# Tip Controls

Effect of Mach number. A comparison of the variations of hingemoment coefficient with control deflection at M = 1.61 and M = 2.01 is shown in figure 15 for configurations A, E, F, and G. The data at M = 1.61 were taken from reference 1. In general, the shapes of the curves are very similar at the two Mach numbers, and the primary effect of increasing Mach number is to cause considerable decrease in the slopes of the curves for configurations A and E, and some small decrease in the slope for configuration F. The change in slope near  $\alpha=0^{\circ}$  and  $\delta=0^{\circ}$  was negligible for configuration G.

The theoretical and experimental variations of  $(c_{h,l})_{\delta}$  and  $(c_{h,l})_{\alpha}$  with Mach number for configurations A, E, F, and G are shown in figure 16. The theoretical values of  $(c_{h,l})_{\delta}$  for all the configurations and of  $(c_{h,l})_{\alpha}$  for configuration A were obtained from the linear-theory equations given in references 6 and 7. The theoretical values of  $(c_{h,l})_{\alpha}$  for configurations E, F, and G were obtained by integrating the theoretical pressure distributions which, in turn, were computed from the equations given in reference 8. The variations of the experimental hingemoment-slope parameters with Mach number are generally in agreement with theory although considerably more positive. Configurations F and G, the most nearly balanced of the aforementioned four controls, exhibit little change in hinge-moment-curve slope with Mach number in this range.

In reference 1, correlations of the hinge-moment-slope parameters with the ratio of control balance area to control total area were obtained for a series of tip controls on the present wing at M=1.61. Figure 17 presents similar correlations obtained during the present tests at M=2.01 for four of the tip controls. These correlations again show that a balanced tip control with desired low-angle hingemoment slopes may be obtained by proper selection of the ratio of control balance area to total area.

Effect of offsetting tip control.— Configuration H is the control of configuration F with its torque tube inserted in the hinge-line hole of configuration E. The effects of offsetting the tip control with respect to the main wing on the hinge-moment characteristics are shown in figure 18 where the hinge-moment-coefficient variations for configuration H are compared with those for configuration F. Offsetting the control had little effect on the variation of hinge-moment coefficient with control deflection but caused some increase in slope of the hinge-moment-coefficient curves with angle of attack.

Effect of control plan form.— In reference 1, it was shown that configurations D and F, each with ratios of control balance area to total area of 0.36, had approximately the same hinge-moment characteristics. Both configurations had tip controls; however, configuration D had a more forward hinge-line location, and some of the trailing-edge portion of the control had been removed. Since plan form seemed to have a negligible effect on the hinge-moment characteristics, configuration K, with a rectangular overhang but again with a ratio of control balance area to total area of 0.36, was added to the present tests.

In figure 19, the variations of hinge-moment coefficient with control deflection and angle of attack are presented for configurations D, F, and K. From these curves, it is evident that the plan form of configuration K does not alleviate any of the hinge-moment problems presented by the other closely balanced controls. Both the nonlinearities and regions of overbalance are present in the variations with control deflection for configuration K. At angles of attack, the balancing effectiveness in the negative control-deflection range is greater for configuration K than for configurations D and F. In the variations of hinge-moment coefficient with angle of attack, configuration K produced increased slopes at the negative control deflections because of the strong balancing in this range.

Effect of inset and detached tabs .- The variations of hinge-moment coefficient with control deflection for configuration E with the inset or detached tabs, shown in figures 6 and 7, respectively, indicate that tab deflection caused a general shift in the curves and did not alter the slopes of the variations with control deflection or angle of attack. The incremental hinge-moment-curve slopes due to the addition of tabs to the basic configuration E are plotted in figure 20(a), together with the values obtained from the attached-tab tests of reference 2, as a function of the tab-area moment about the control hinge line. The variation of hinge-moment-coefficient slope due to tab deflection with tab-area moment shows an increasing trend greater than that of the linear variation found for attached tabs on a sweptforward trailing edge as in reference 9. This effect is contrary to the effect which would be anticipated theoretically since the inset tab should produce some additional hinge moment from the load induced on the adjacent control surface.

The curves of incremental hinge-moment-coefficient slope with control deflection and angle of attack due to the addition of tabs (fig. 20(a)) show that, as anticipated, the inset tab causes no increments. The detached tab caused considerably more change in  $\binom{C}{h,l}_{\alpha}$  than did the attached tab but caused only slightly more change in  $\binom{C}{h,l}_{\delta}$ .

NACA RM L57BO1

In order to evaluate the various tabs as devices for balancing the control hinge moments, the ratio of tab deflection to control deflection required for  $(C_{h,l})_{\delta} = 0$  is plotted in figure 20(b) as a function of angle of attack for the inset and detached tabs of the present tests and for the two sizes of attached tabs of reference 2. From these curves it is evident that the detached tab was the most effective device in balancing the hinge moments due to control deflection. The detached tab would probably cause the least reduction in control effectiveness but

the largest penalty in drag of the three types of tabs listed.

Effect of fixed tab on a boom. In reference 1, the detrimental effects of closely balancing the hinge moments due to control deflection were the increased nonlinearities in the curves and regions of overbalance. Configuration E-1 was designed by adding a fixed tab on a boom to the control of configuration E. The tab size and location were selected so that configuration E-1 had the same net control-area moment about the hinge line as configuration F had. The hinge-moment-coefficient variations with control deflection and angle of attack for configurations E-1 and F are presented in figure 21. At the positive control deflections, the two configurations are very nearly alike; however, at the low and negative control deflections with the wing at angles of attack, the tab configuration exhibits more negative hinge-moment coefficients apparently because of a strong downward force imposed on the tab by the very complicated flow field through which it operates.

Effect of fences .- A comparison of the effect of the three fences on the hinge-moment-coefficient variations with control deflection and angle of attack for configuration F are shown in figure 22. Configuration F-3 is apparently the most beneficial fence configuration because it reduces the hinge-moment coefficient due to control deflection at low angles of attack and decreases the nonlinearities at the higher angles of attack. In order to compare the effect of fences on the hinge-moment characteristics of configuration F with the effects previously presented in reference 2 of similar fences on a more unbalanced control configuration E, curves of the incremental hinge-moment coefficient due to the fences with control deflection are plotted in figure 23. In figure 23(a), the fullchord fences are compared and in figure 23(b), the partial-chord fences are compared. The incremental hinge-moment-coefficient variations are very much alike for similar fences on the two configurations. Analysis of the pressure distributions (tabulated in ref. 5) indicates that the differences shown in figure 23 for similar fences can be explained on the basis of the hinge-line movement and the elimination by the fences of the induced crossflows present at the parting line in the basic configurations.

# Trailing-Edge Controls

Effect of span and location. Comparison of the hinge-moment-coefficient variations with control deflection and angle of attack for configuration I of the present tests with those for configuration A of reference 1 and configuration J of reference 3 is made in figure 24. Configurations I and J exhibit marked decreases in hinge-moment-curve slope with control deflection at the highest control deflections, whereas the curves for configuration A are generally linear throughout the test range. This decrease in slope probably can be attributed to a greater viscous effect over the inboard stations of the wing because of the change in airfoil section. Over the span of the inboard control, the trailing-edge wedge is preceded by a flat section, whereas over the span of the outboard control, the rounded leading-edge section is followed immediately by the trailing-edge wedge.

In general, the curves show considerable effects of both span and spanwise location of the trailing-edge controls on the slopes of the curves with both control deflection and angle of attack. These results are contrary to the results shown in reference 10 for trailing-edge controls on a trapezoidal wing wherein  $\binom{C_h}{\delta}$  was relatively unaffected

by changes in span or spanwise location. The effects found herein are, however, in agreement with the trends predicted by the linear theory method of reference 6. Table I shows that the experimental parameters are approximately 70 percent of the theoretical values as was the case in reference 10, but the differences in the experimental slopes with changes in control span or location are in the same direction as the theoretical predictions. Configuration J, with the largest amount of essentially two-dimensional flow, produced the greatest  $(C_h)_8$ , and con-

figuration A, with the least amount of two-dimensional flow produced the least  $(C_h)_\delta$ . Configuration A, operating in the region of high loading near the leading edge due to angle of attack, produced the greatest  $(C_h)_\alpha$  and configuration I, operating wholly inboard, produced the least  $(C_h)_\alpha$ .

Effect of spanwise location of tabs.— The hinge-moment-coefficient variation with control deflection for the inboard attached tab on configuration J (fig. 11) shows little effect of tab deflection. The slopes of the hinge-moment curves with control deflection are the same for the inboard tab (fig. 11) as for the outboard tab (fig. 12). Crossplots of the hinge-moment coefficients with tab deflection, however, show that the outboard tab is more effective in producing hinge moment with tab deflection. The ratio of tab deflection to control deflection required for  $C_{h,\delta}=0$  is plotted against angle of attack in figure 25 and shows that the net result is a lower value of  $\delta_t/\delta$  for the outboard tab. In reference 9, it was predicted that an outboard tab would be more effective

NACA RM L57B01

as a balancing device on a control with an unswept trailing edge, but it is interesting to note that the reasons given therein do not coincide with the experimental effects found in the present investigation. It was anticipated that  $C_{h,\delta_t}$  would be the same for the two tabs and  $C_{h,\delta}$  would be smaller for the outboard tab, whereas the present tests showed equal values of  $C_{h,\delta}$  and greater values of  $C_{h,\delta_t}$  for the outboard tab. The discrepancy is undoubtedly caused by the difference in wing plan form and the large spanwise variation in the strength of viscous effects on the delta wing.

Effect of trailing-edge thickness. The variations of hinge-moment coefficient with control deflection and angle of attack for the thickened trailing-edge configurations J-1 and J-2 are compared with the variations for the sharp trailing-edge configuration J from reference 3 in figure 26. As the control trailing-edge thickness increases, the slope of the hinge-moment-coefficient curves with control deflection increases. At  $\delta=0^{\circ}$ ,  $-15^{\circ}$ , and  $-30^{\circ}$ , the slope of the hinge-moment-coefficient curves with angle of attack also increased with increasing trailing-edge thickness. The increases in hinge-moment-curve slopes with increasing trailing-edge thickness are approximately linear. These increases are in agreement with the theoretical prediction of the effect of increasing control trailing-edge thickness shown in reference 10 and with the experimental pressure-distribution analysis of reference 11. It should be mentioned that increasing the control trailing-edge thickness also increases the control effectiveness. (See ref. 10.)

Effect of paddle balances. The hinge-moment-coefficient variations with control deflection and angle of attack for configuration J-3 with the paddle balances and the variations for the basic configuration J from reference 3 are presented in figure 27. The paddle balances were effective in reducing the hinge moments due to control deflection but had little effect on the curve slopes of the hinge-moment coefficient with angle of attack. This effect is in agreement with the results previously obtained on paddle balances in reference 12.

### CONCLUSIONS

An investigation has been made at Mach numbers of 1.61 and 2.01 to determine the hinge-moment characteristics for a series of 18 controls, including the effects of various tabs and fences, on a 60° delta wing. Tests were made at angles of attack from 0° to 12°, for control deflections from -30° to 30°, and for tab deflections from 0° to -20°. The results indicate the following primary conclusions:

NACA RM L57BOl

1. Correlations of the hinge-moment-slope parameters with the ratio of the balance area to the total area of the control were obtained for a series of tip controls at a Mach number of 2.01 similar to those correlations previously obtained at a Mach number of 1.61.

- 2. Variation of the hinge-moment-slope parameters for trailing-edge controls with span and spanwise location were similar to the theoretical predictions; however, the absolute values of the experimental hinge-moment-slope parameters were about 70 percent of the theoretical values.
- 3. Increasing the trailing-edge thickness generally increased the hinge-moment-slope parameters on the full-span trailing-edge control.
- 4. A parting-line fence forward of the hinge line on a closely balanced tip control resulted in improved hinge-moment characteristics similar to the improvements previously found in tests of more unbalanced tip controls.
- 5. A detached tab on a tip control was more effective in balancing the hinge moments due to control deflection than either an inset or attached tab.
- 6. An attached tab on a full-span trailing-edge control was more effective in balancing the hinge moments due to control deflection when located outboard than when located inboard.
- 7. Paddle balances on a full-span trailing-edge control decreased the slope of the hinge-moment-coefficient variation with control deflection but had little effect on the slope of the hinge-moment-coefficient variation with angle of attack.

Langley Aeronautical Laboratory,
National Advisory Committee for Aeronautics,
Langley Field, Va., January 11, 1957.

#### REFERENCES

- 1. Czarnecki, K. R., and Lord, Douglas R.: Hinge-Moment Characteristics for Several Tip Controls on a 60° Sweptback Delta Wing at Mach Number 1.61. NACA RM L52K28, 1953.
- 2. Czarnecki, K. R., and Lord, Douglas R.: Preliminary Investigation of the Effect of Fences and Balancing Tabs on the Hinge-Moment Characteristics of a Tip Control on a 60° Delta Wing at Mach Number 1.61.

  NACA RM L53D14, 1953.
- 3. Lord, Douglas R., and Czarnecki, K. R.: Aerodynamic Characteristics of a Full-Span Trailing-Edge Control on a 60° Delta Wing With and Without a Spoiler at a Mach number of 1.61. NACA RM L53L17, 1954.
- 4. Lord, Douglas R., and Czarnecki, K. R.: Aerodynamic Characteristics of Several Tip Controls on a 60° Delta Wing at a Mach Number of 1.61. NACA RM L54E25, 1954.
- 5. Lord, Douglas R., and Czarnecki, K. R.: Tabulated Pressure Data for a Series of Controls on a 60° Delta Wing at Mach Numbers of 1.61 and 2.01. NACA RM L55L05, 1956.
- 6. Tucker, Warren A., and Nelson, Robert L.: Theoretical Characteristics in Supersonic Flow of Two Types of Control Surfaces on Triangular Wings. NACA Rep. 939, 1949. (Supersedes NACA TN's 1600 and 1601 by Tucker and TN 1660 by Tucker and Nelson.)
- 7. Kainer, Julian H., and King, Mary Dowd: The Theoretical Characteristics of Triangular-Tip Control Surfaces at Supersonic Speeds. Mach Lines Behind Trailing Edges. NACA TN 2715, 1952.
- 8. Martin, John C., Margolis, Kenneth, and Jeffreys, Isabella: Calculation of Lift and Pitching Moments Due to Angle of Attack and Steady Pitching Velocity at Supersonic Speeds for Thin Sweptback Tapered Wings With Streamwise Tips and Supersonic Leading and Trailing Edges. NACA TN 2699, 1952.
- 9. Lord, Douglas R., and Driver, Cornelius: Investigation of the Effect of Balancing Tabs on the Hinge-Moment Characteristics of a Trailing-Edge Flap-Type Control on a Trapezoidal Wing at a Mach Number of 1.61. NACA RM L54F22, 1954.
- 10. Lord, Douglas R., and Czarnecki, K. R.: Aerodynamic Characteristics of Several Flap-Type Trailing-Edge Controls on a Trapezoidal Wing at Mach Numbers of 1.61 and 2.01. NACA RM L54D19, 1954.

NACA RM L57B01 13

11. Lord, Douglas R., and Czarnecki, K. R.: Pressure Distributions and Aerodynamic Loadings for Several Flap-Type Trailing-Edge Controls on a Trapezoidal Wing at Mach Numbers of 1.61 and 2.01. NACA RM L55J03, 1956.

12. Boyd, John W., and Pfyl, Frank A.: Experimental Investigation of Aerodynamically Balanced Trailing-Edge Control Surfaces on an Aspect Ratio 2 Triangular Wing at Subsonic and Supersonic Speeds. NACA RM A52LO4, 1953.

TABLE I.- HINGE-MOMENT-COEFFICIENT SLOPES
FOR THREE TRAILING-EDGE CONTROLS

М	Configuration	C <sub>h</sub> ,	δ	C <sub>h,a</sub>					
	Ooiii igai a oi oii	Experiment	Theory	Experiment	Theory				
	A	-0.0168	-0.0239	-0.0240	-0.0341				
1.61	I	0182	0260	0127	0158				
	J	0196	0275	0147	0233				
2.01	A	0130	0187	0180	0295				

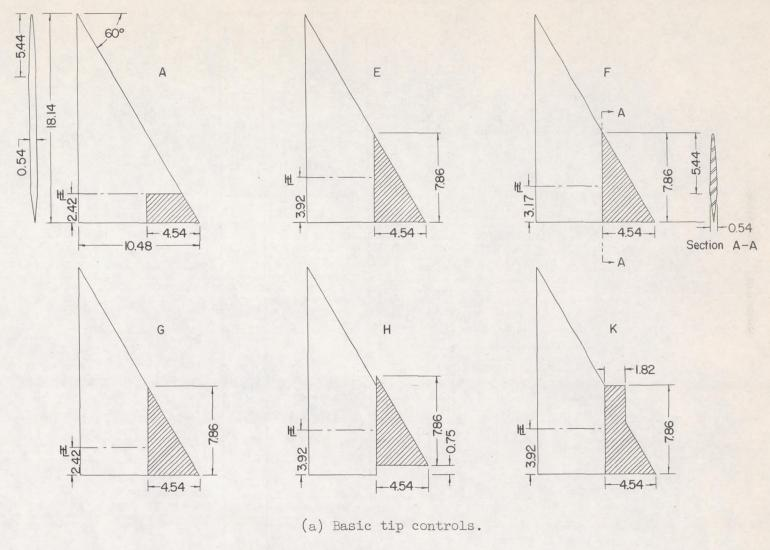
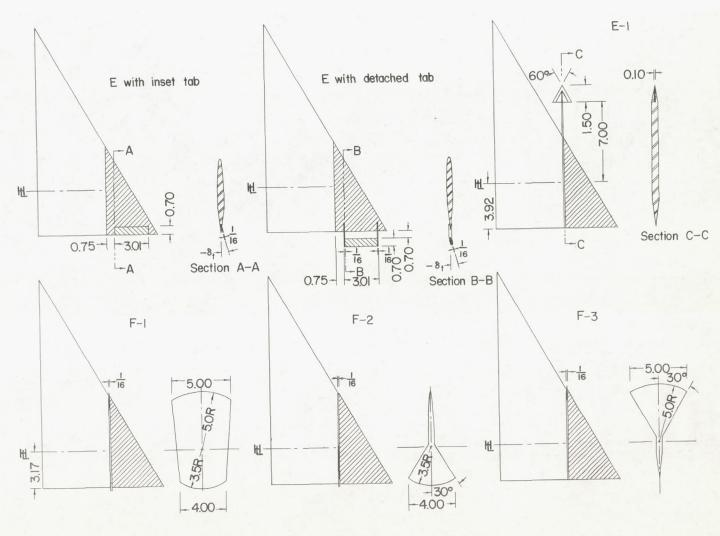
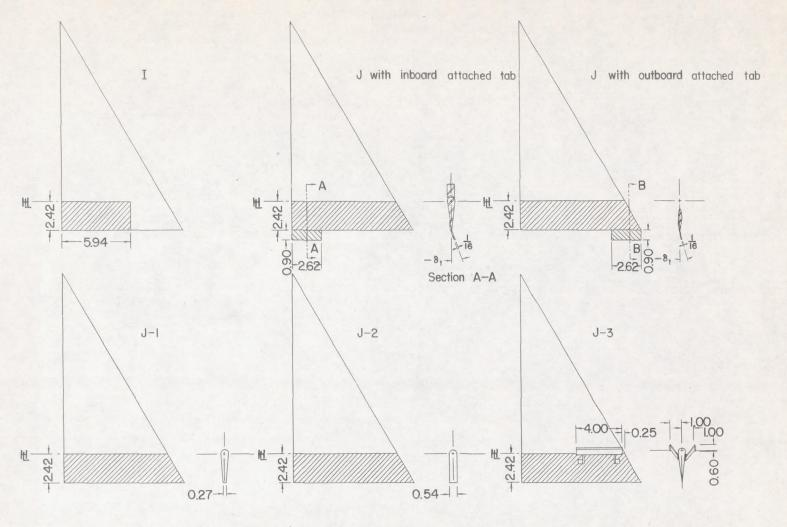


Figure 1.- Sketches of model configurations. All dimensions are in inches.



(b) Tip controls with tabs or fences.

Figure 1. - Continued.



(c) Trailing-edge controls.

Figure 1. - Concluded.

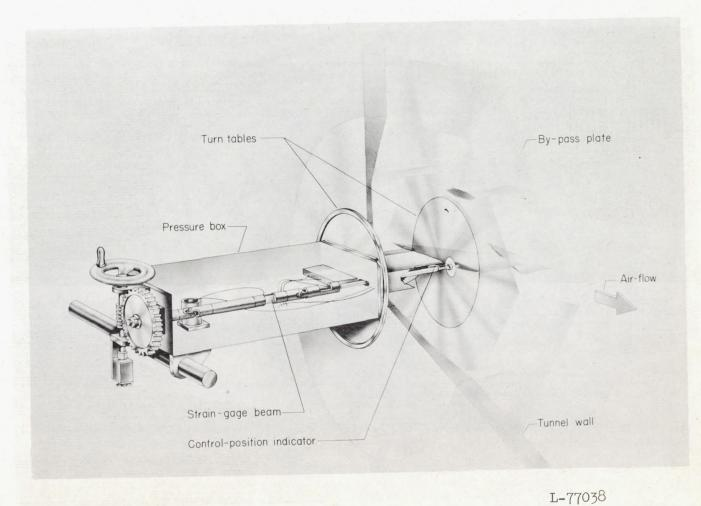


Figure 2.- Sketch of test setup showing one tip control in deflected position.

NACA RM L57B01

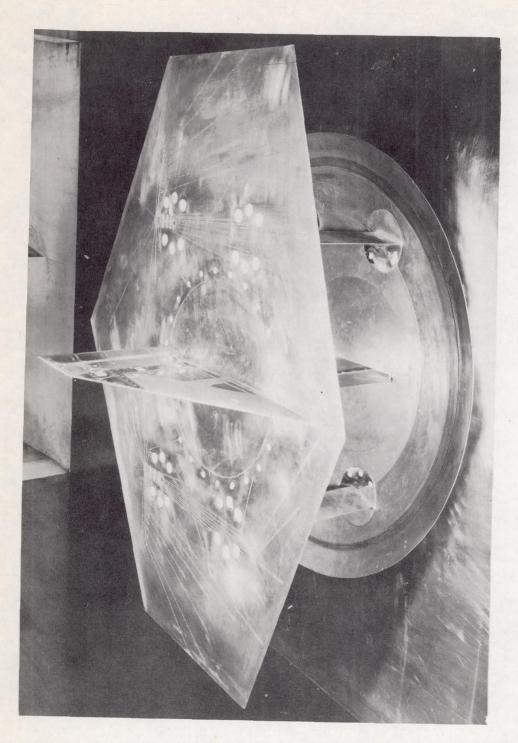
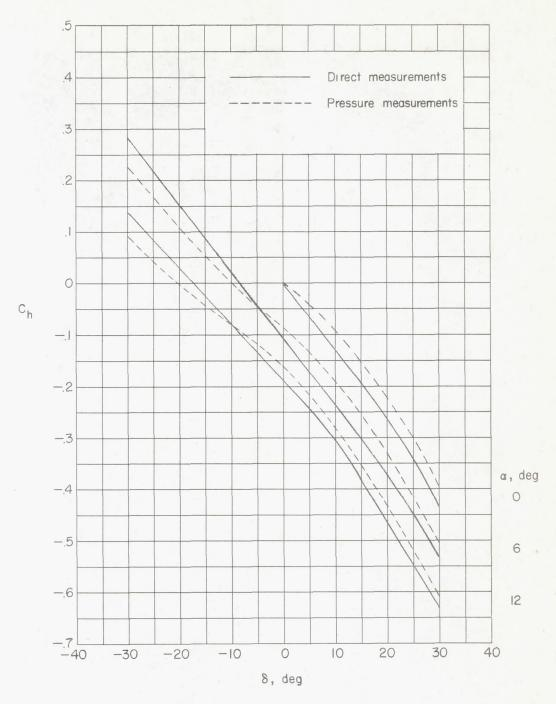
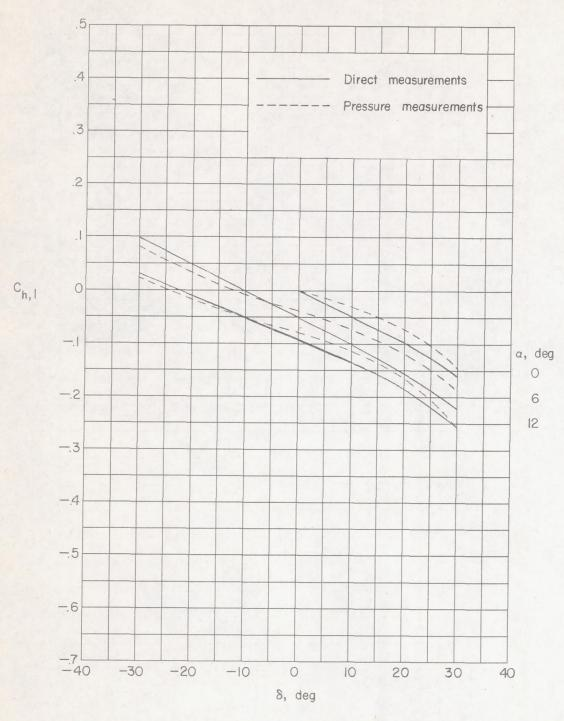


Figure 3.- Photograph of configuration J mounted on boundary-layer bypass plate.



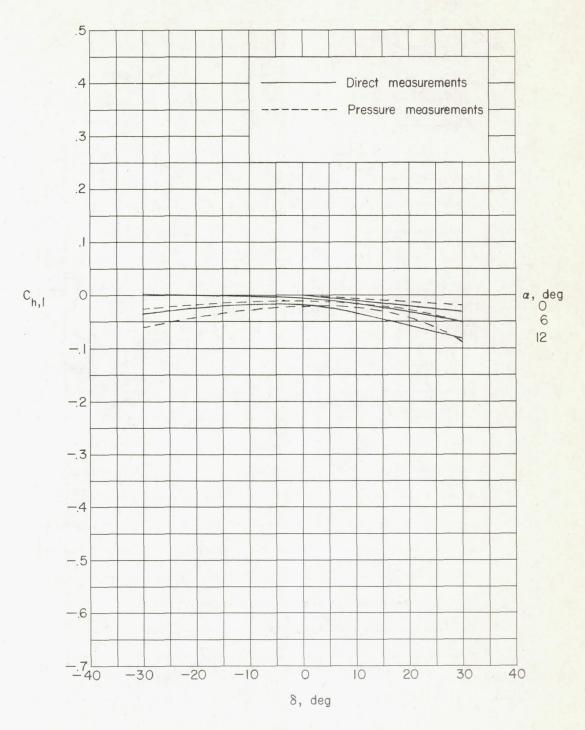
(a) Configuration A.

Figure 4.- Variation of hinge-moment coefficient of control with control deflection for four configurations tested at M = 2.01.



(b) Configuration E.

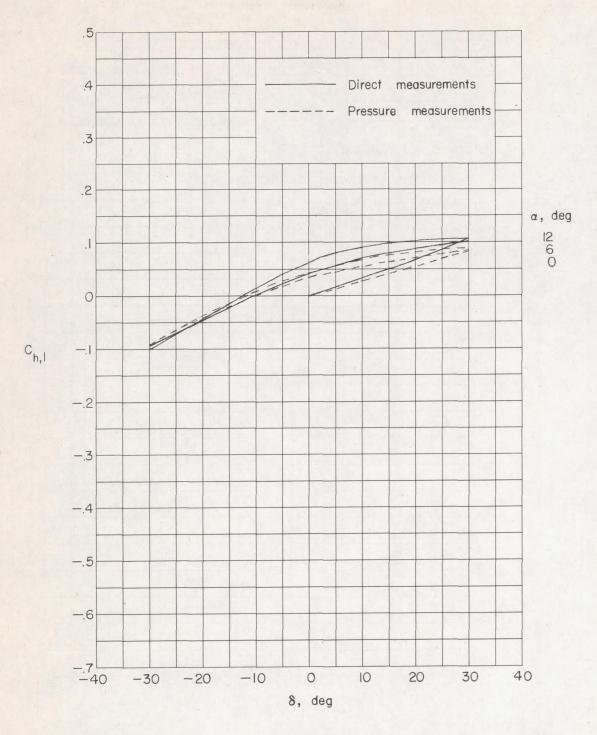
Figure 4. - Continued.



(c) Configuration F.

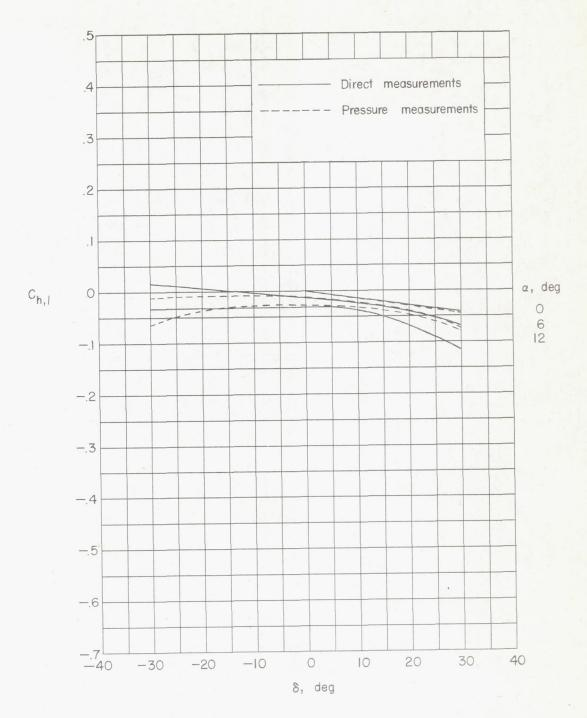
Figure 4.- Continued.

23



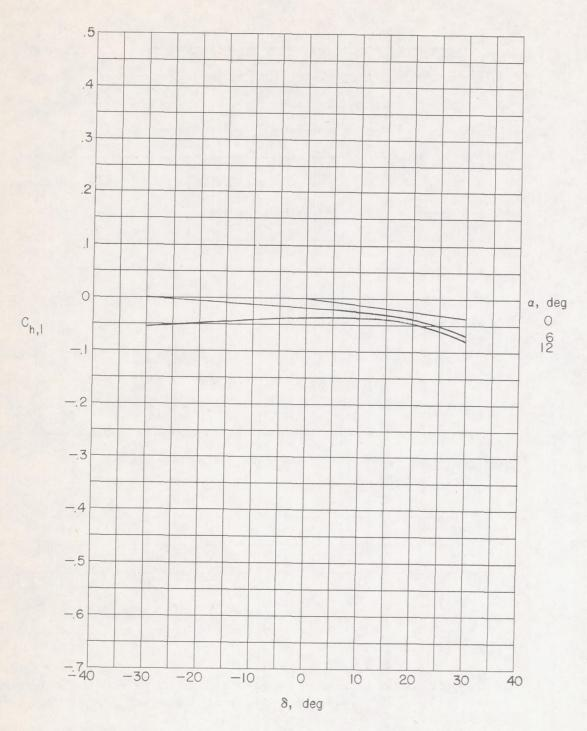
(d) Configuration G.

Figure 4.- Concluded.



(a) Configuration H.

Figure 5.- Variation of hinge-moment coefficient of control with control deflection for two basic tip controls tested at M = 1.61.



(b) Configuration K.

Figure 5.- Concluded.

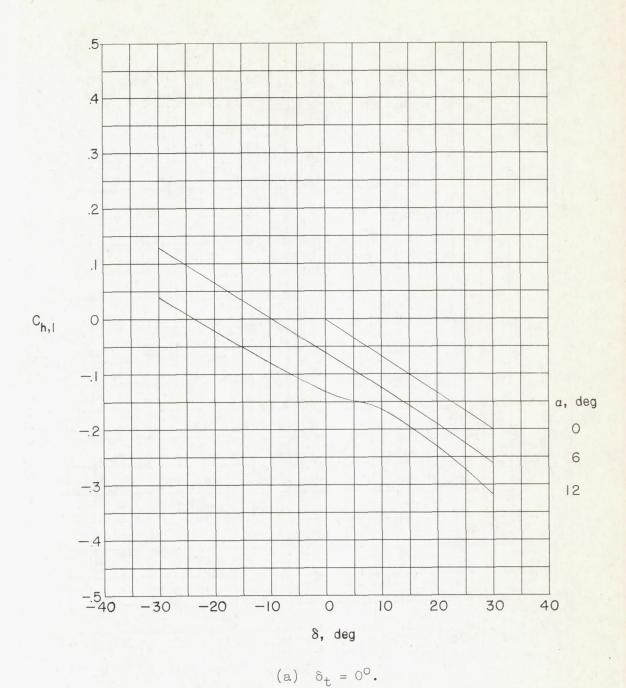
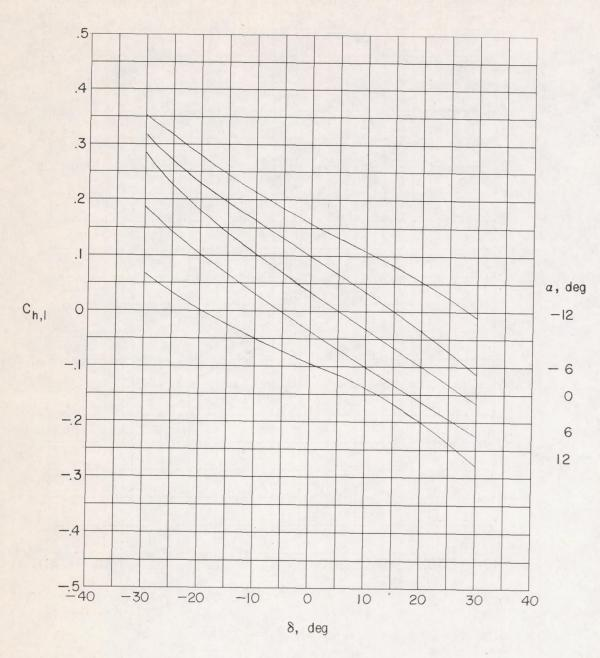
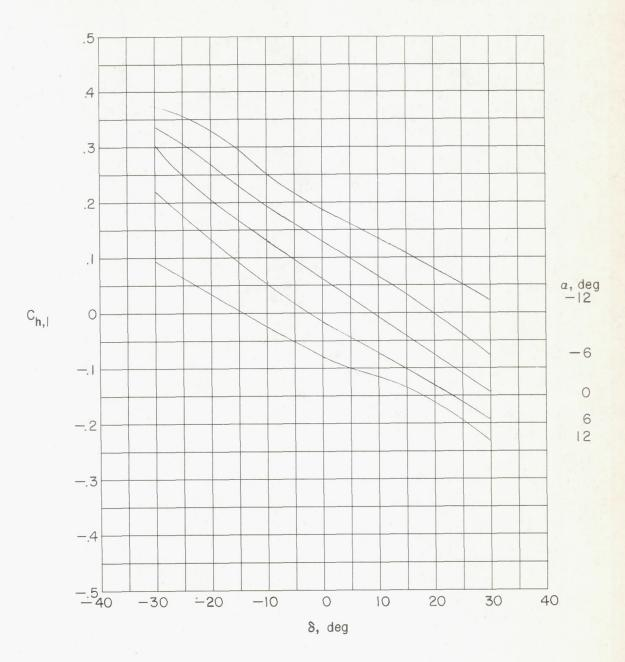


Figure 6.- Variation of hinge-moment coefficient of control with control deflection for configuration E with inset tab. M = 1.61.



(b)  $\delta_{t} = -10^{\circ}$ .

Figure 6.- Continued.



(c)  $\delta_t = -20^\circ$ .

Figure 6.- Concluded.

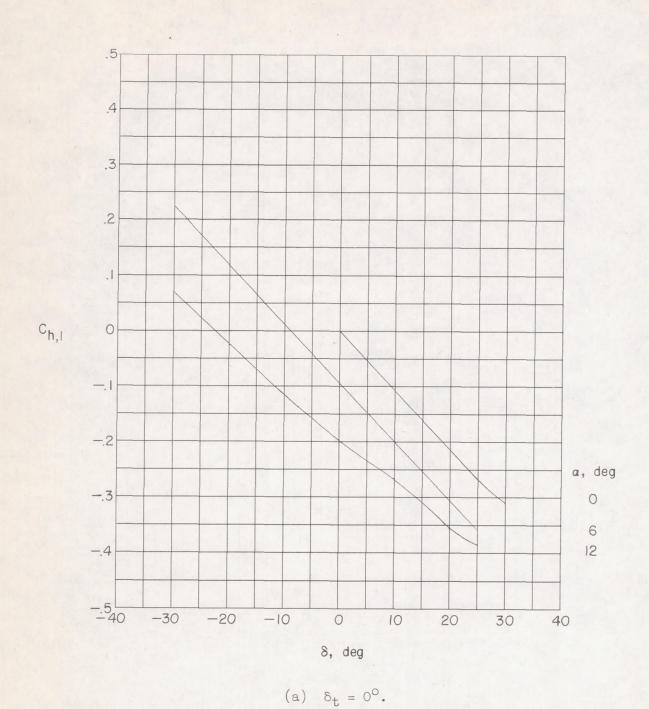


Figure 7.- Variation of hinge-moment coefficient of control with control deflection for configuration E with detached tab. M = 1.61.

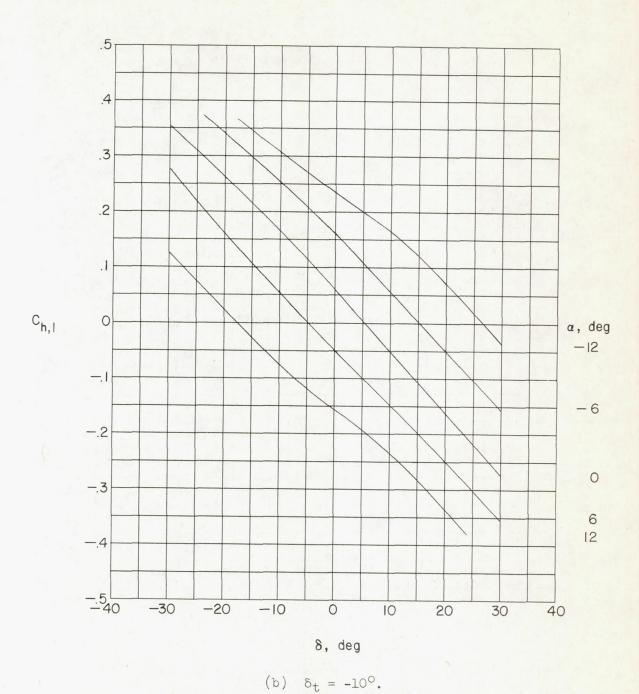
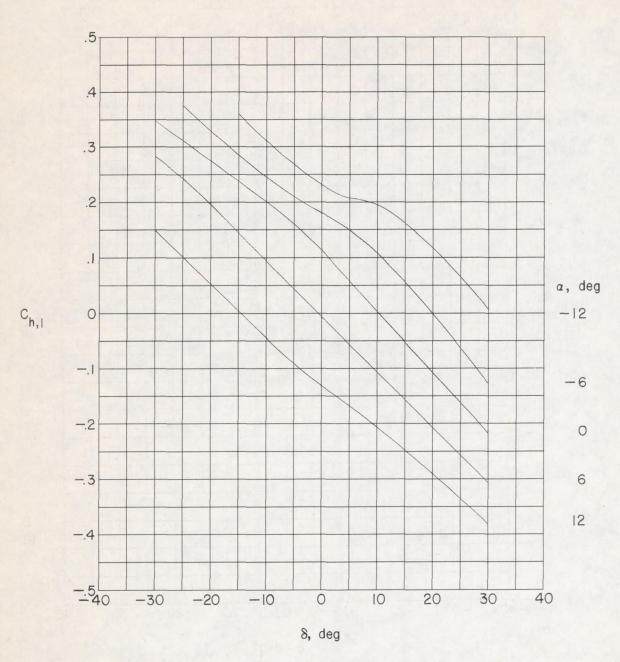


Figure 7.- Continued.



(c)  $\delta_t = -20^\circ$ .

Figure 7.- Concluded.

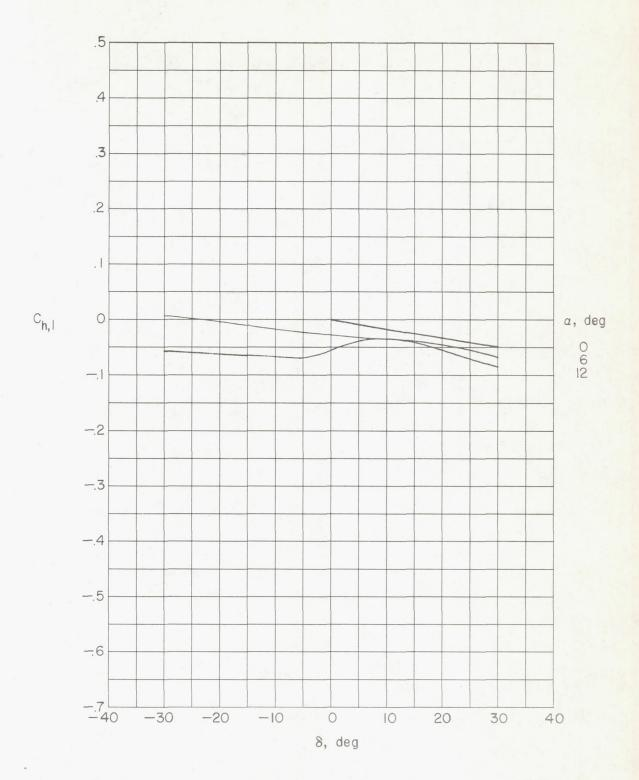
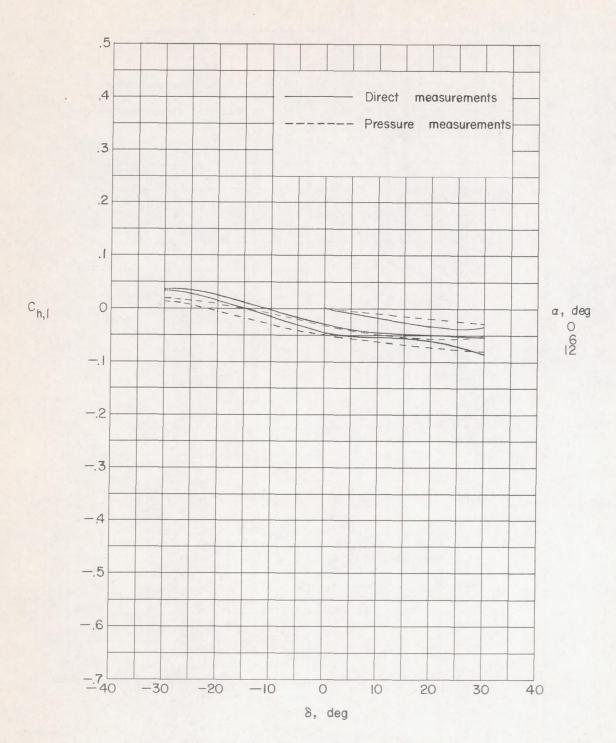
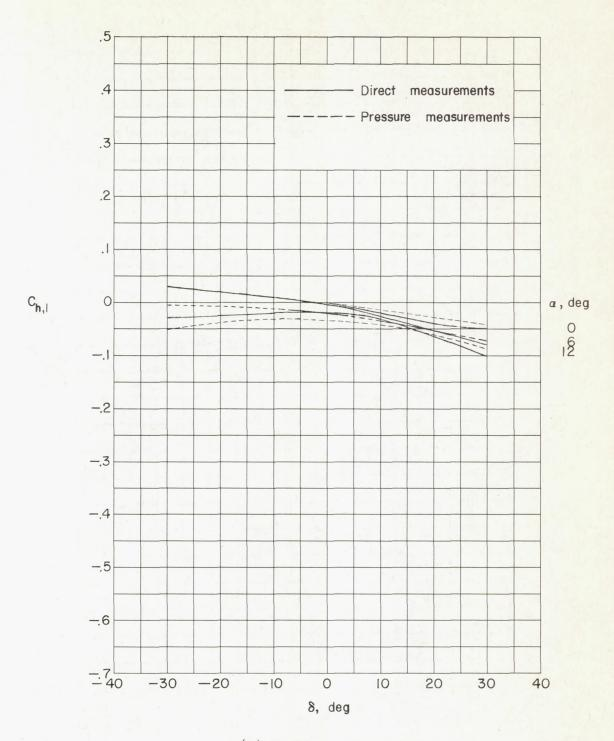


Figure 8.- Variation of hinge-moment coefficient of control with control deflection for configuration E-1. M = 1.61.



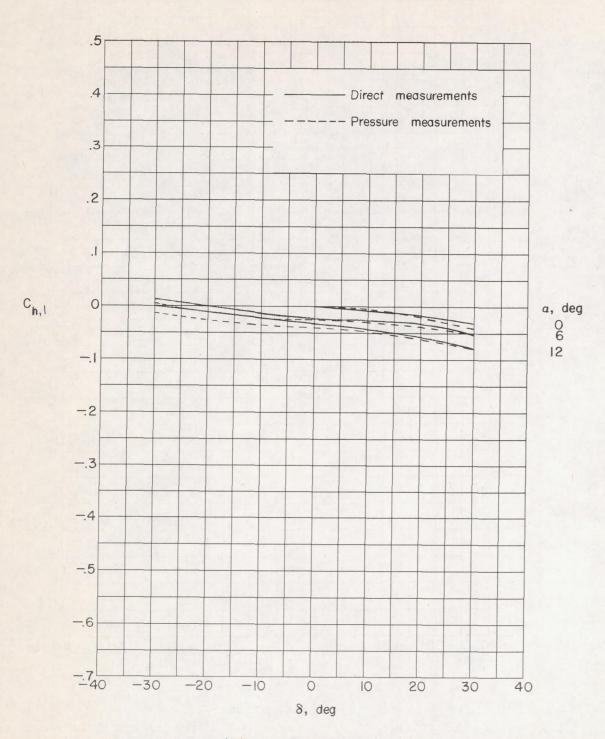
(a) Configuration F-1.

Figure 9.- Variation of hinge-moment coefficient of control with control deflection for three fence configurations. M = 1.61.



(b) Configuration F-2.

Figure 9 .- Continued.



(c) Configuration F-3.

Figure 9. - Concluded.

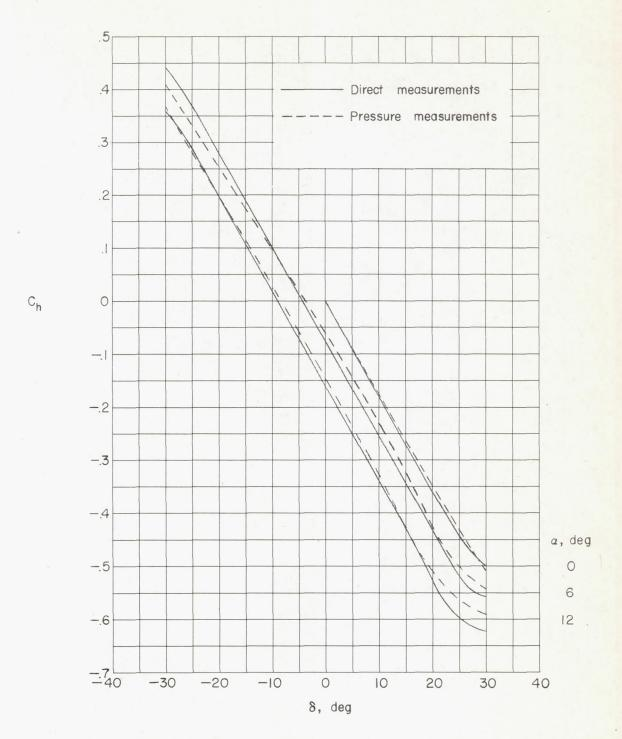


Figure 10.- Variation of hinge-moment coefficient of control with control deflection for configuration I. M = 1.61.

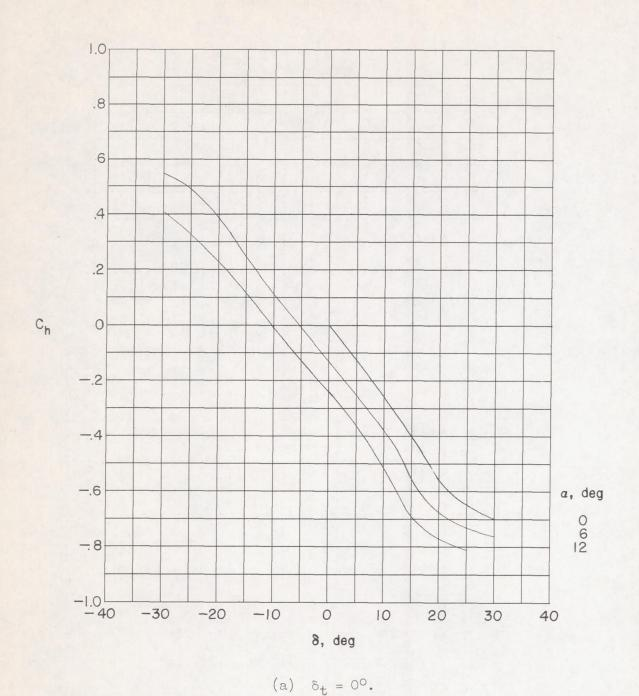
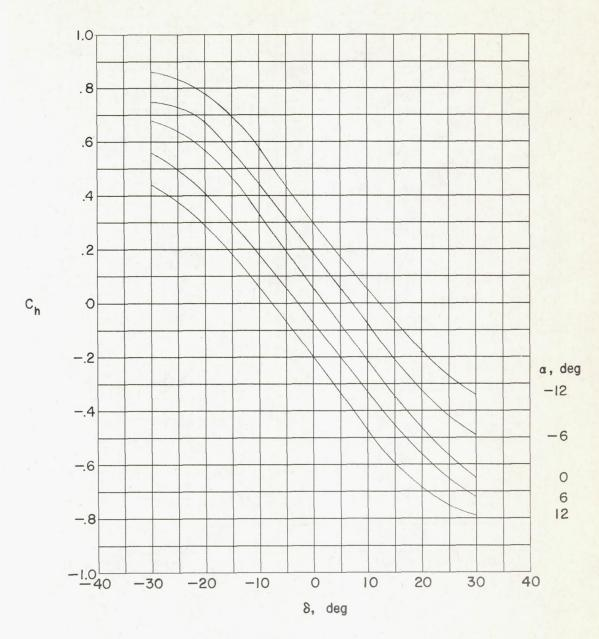
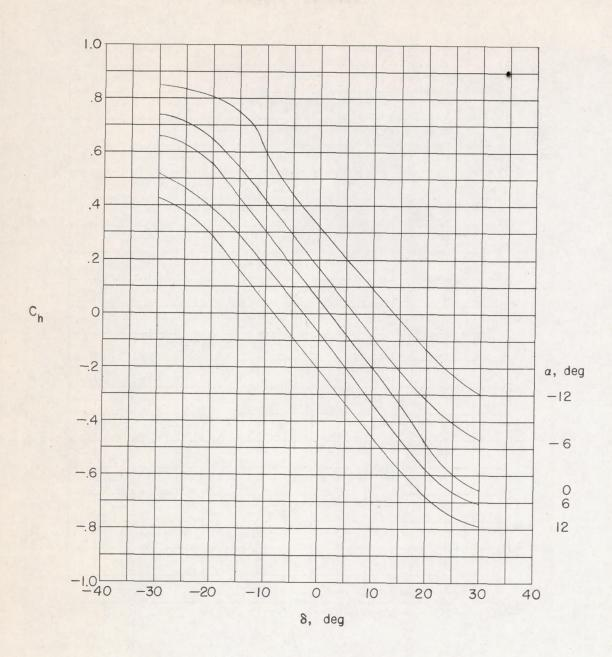


Figure 11.- Variation of hinge-moment coefficient of control with control deflection for configuration J with inboard attached tab. M = 1.61.



(b)  $\delta_{t} = -10^{\circ}$ .

Figure 11. - Continued.



(c) 
$$\delta_t = -19^\circ 5'$$
.

Figure 11. - Concluded.

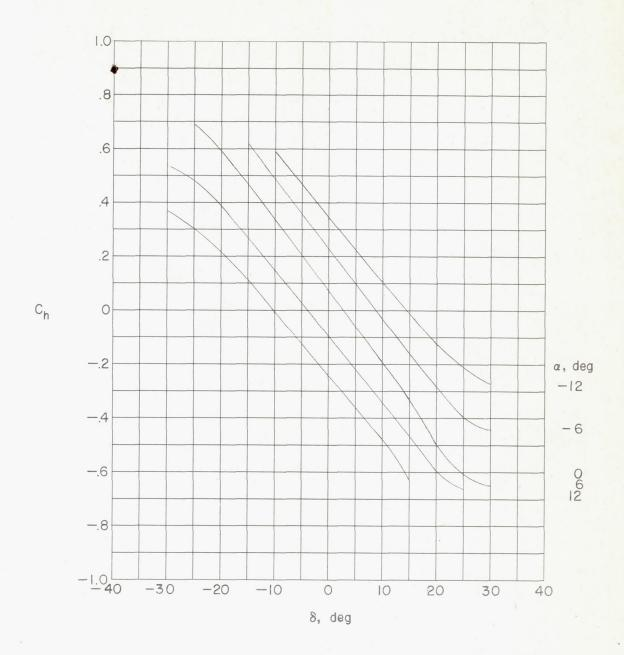
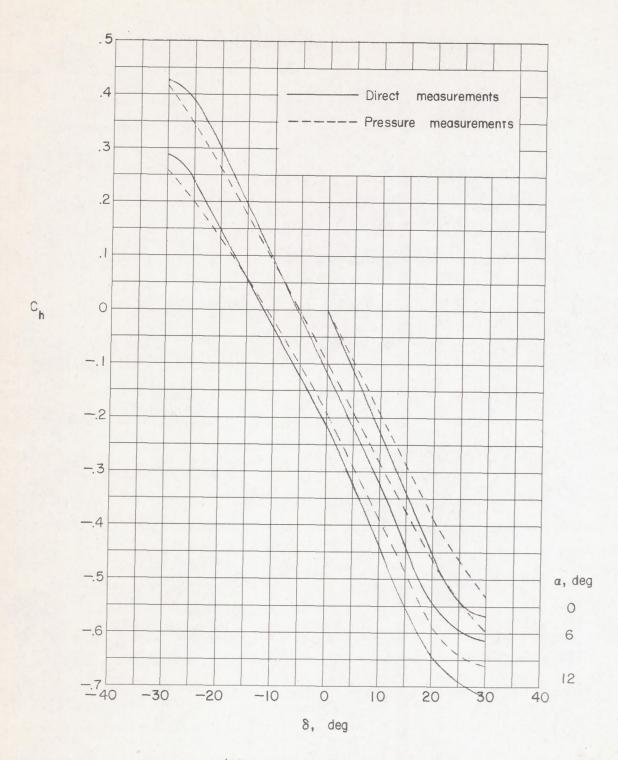
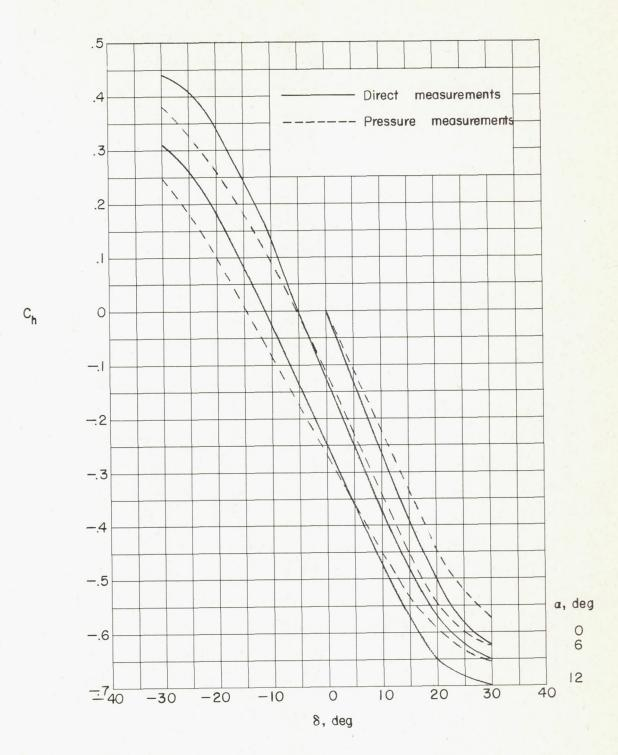


Figure 12.- Variation of hinge-moment coefficient of control with control deflection for configuration J with outboard attached tab. M = 1.61,  $\delta_t$  = -9° 50'.



(a) Configuration J-1.

Figure 13.- Variation of hinge-moment coefficient of control with control deflection for thickened trailing-edge configurations. M = 1.61.



(b) Configuration J-2.

Figure 13.- Concluded.

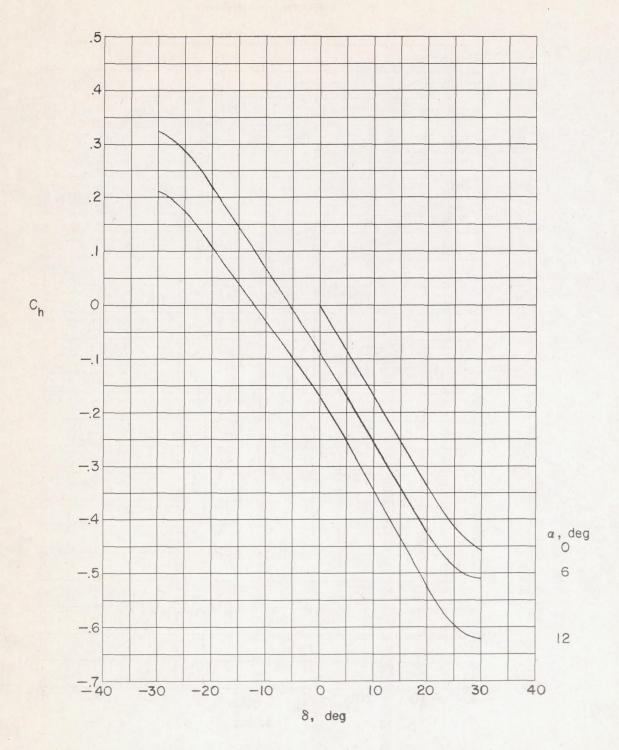
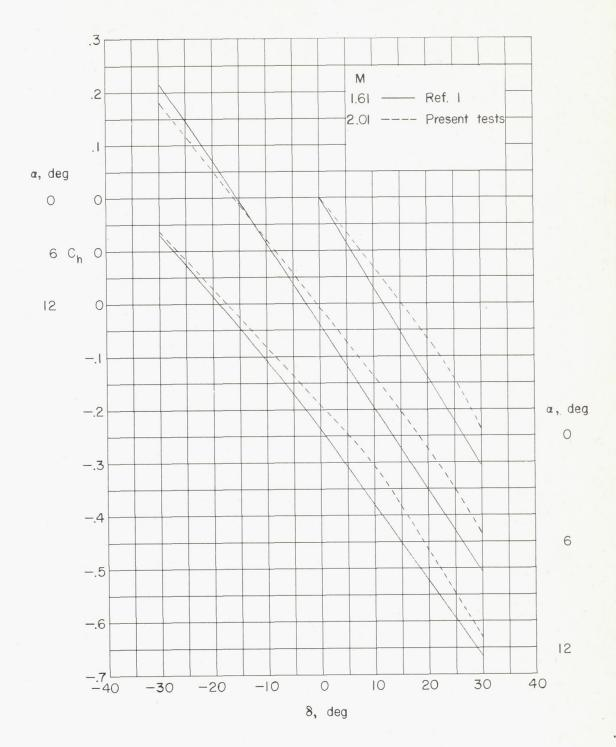
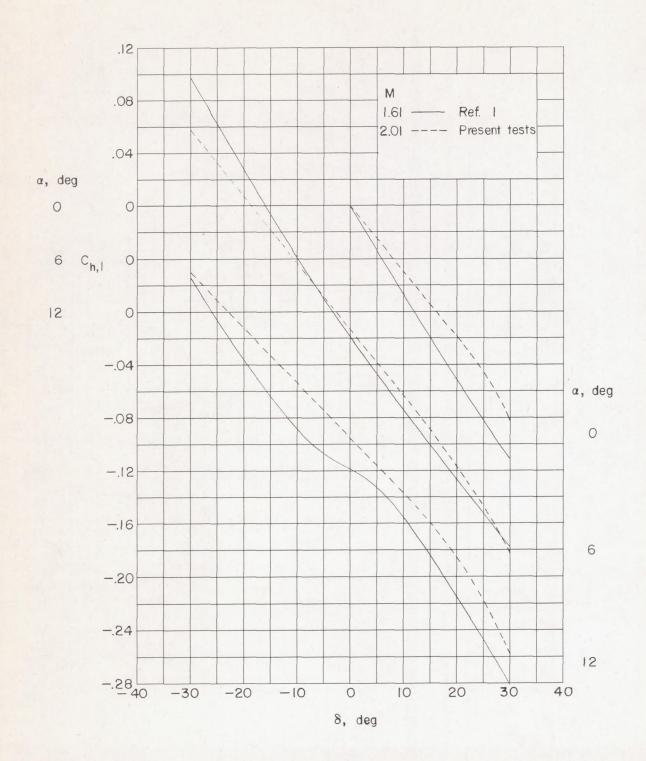


Figure 14.- Variation of hinge-moment coefficient of control with control deflection for configuration J-3. M = 1.61.



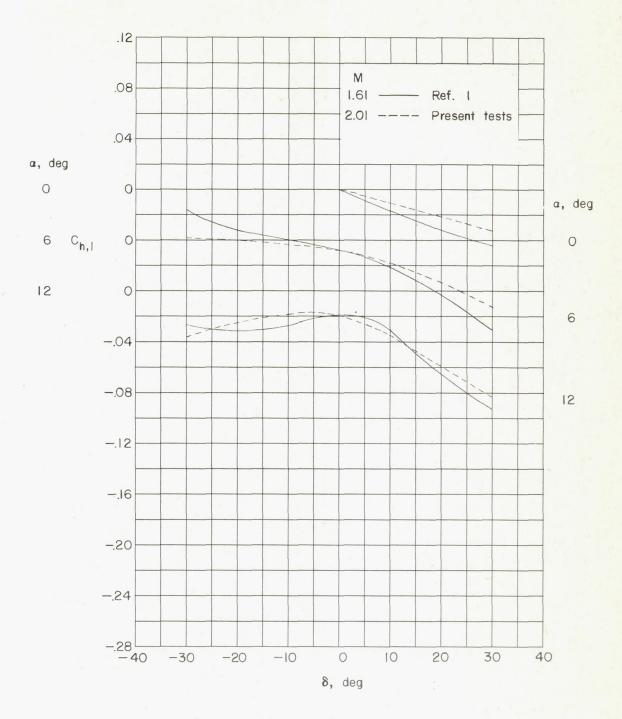
(a) Configuration A.

Figure 15.- Effect of Mach number on hinge-moment-coefficient variations of control with control deflection.



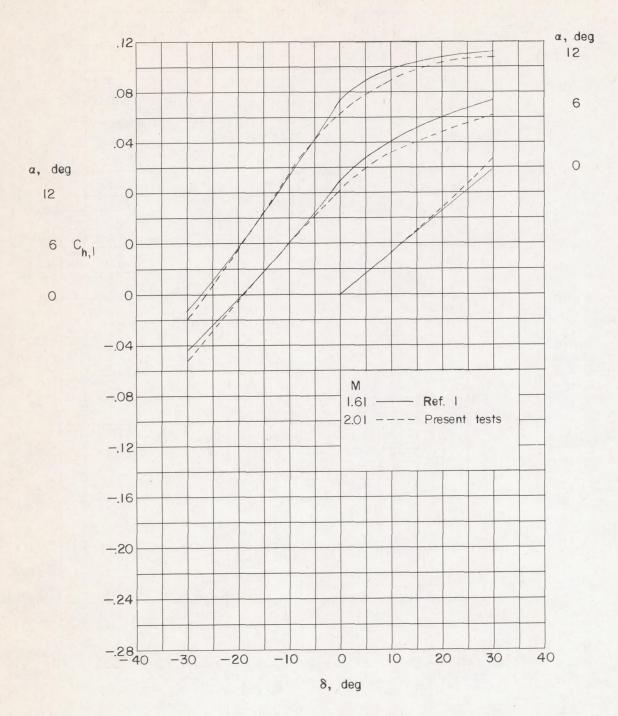
(b) Configuration E.

Figure 15. - Continued.



(c) Configuration F.

Figure 15. - Continued.



(d) Configuration G.

Figure 15.- Concluded.

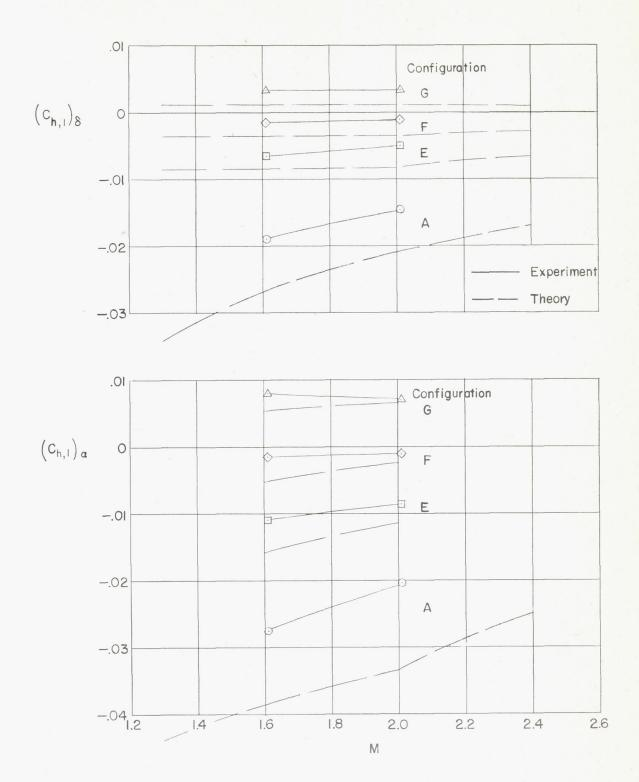


Figure 16.- Variation of hinge-moment-slope parameters of control with Mach number.

-.03

-.04

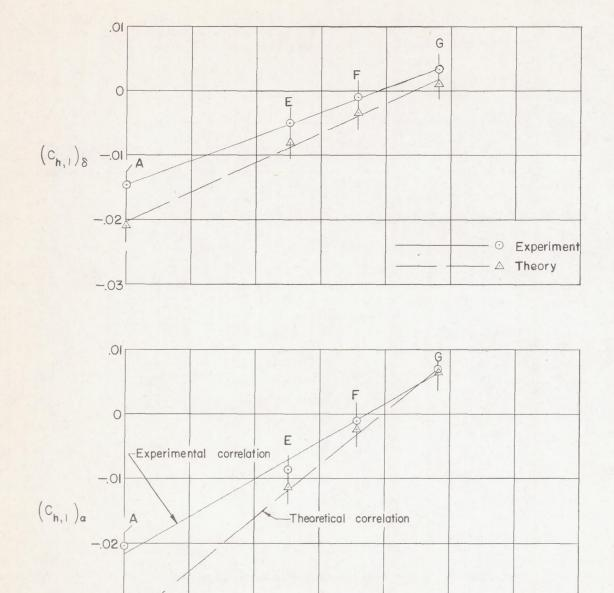


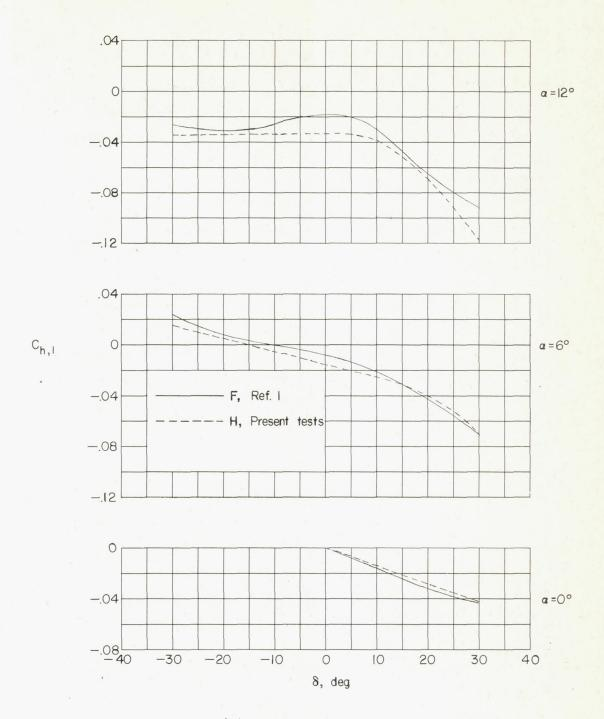
Figure 17.- Correlation of hinge-moment-slope parameters of control with ratio of control balance area to total area. M = 2.01.

.3

.5

.6

.2

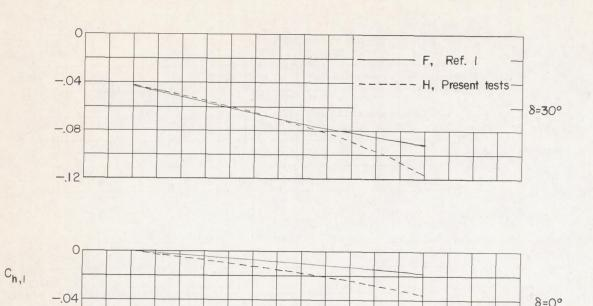


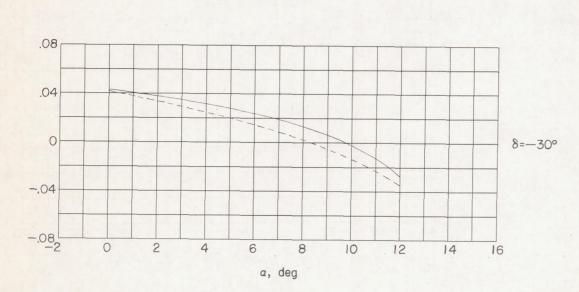
(a) Variation with  $\delta$ .

Figure 18.- Effects of offsetting tip control on hinge-moment-coefficient variations with control deflection and angle of attack. M = 1.61.

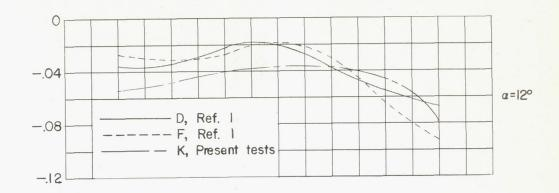
-.08

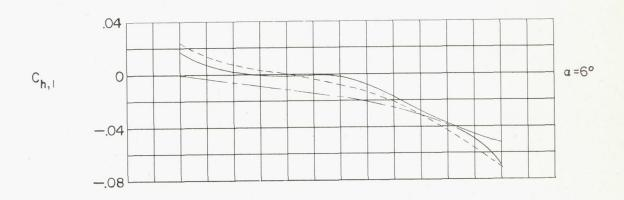
8=0°

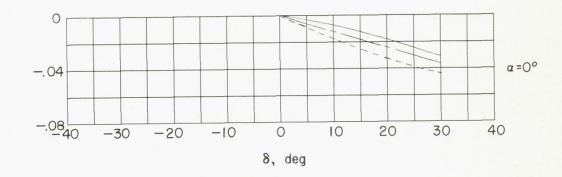




(b) Variation with a. Figure 18. - Concluded.



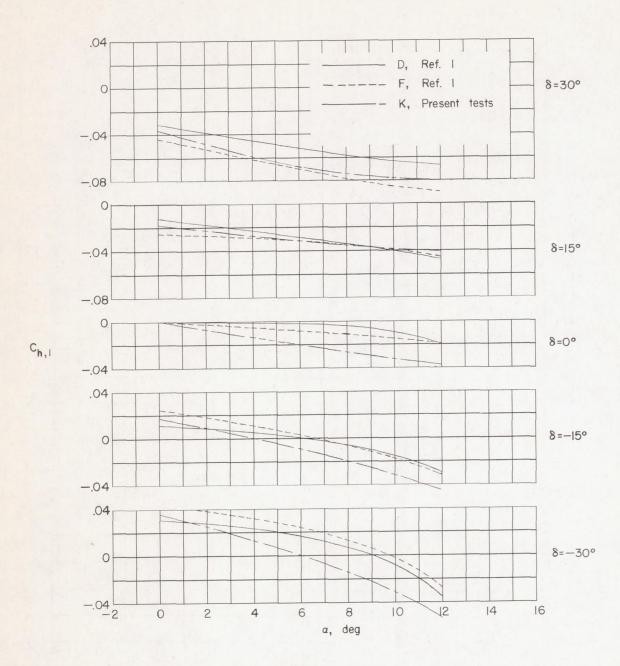




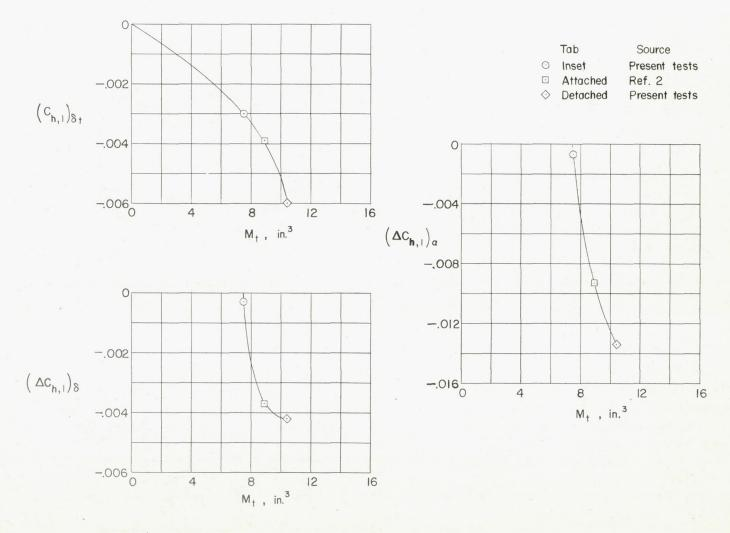
(a) Variation with  $\delta$ .

Figure 19.- Effect of tip-control plan form on hinge-moment-coefficient variations of control with control deflection and angle of attack.

M = 1.61.

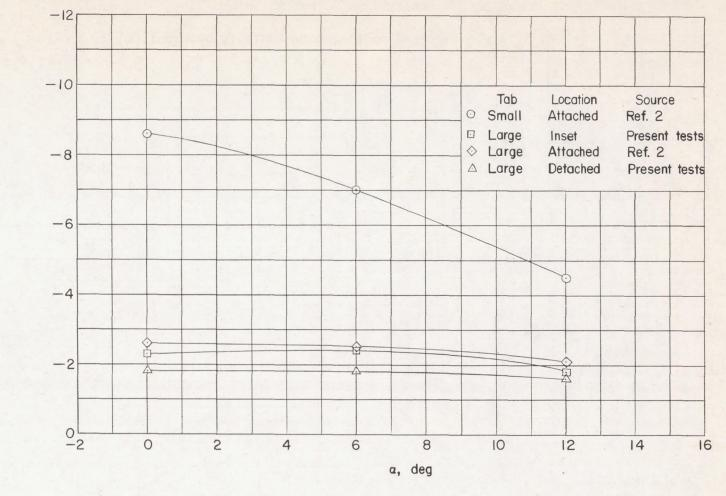


(b) Variation with  $\alpha$ . Figure 19.- Concluded.



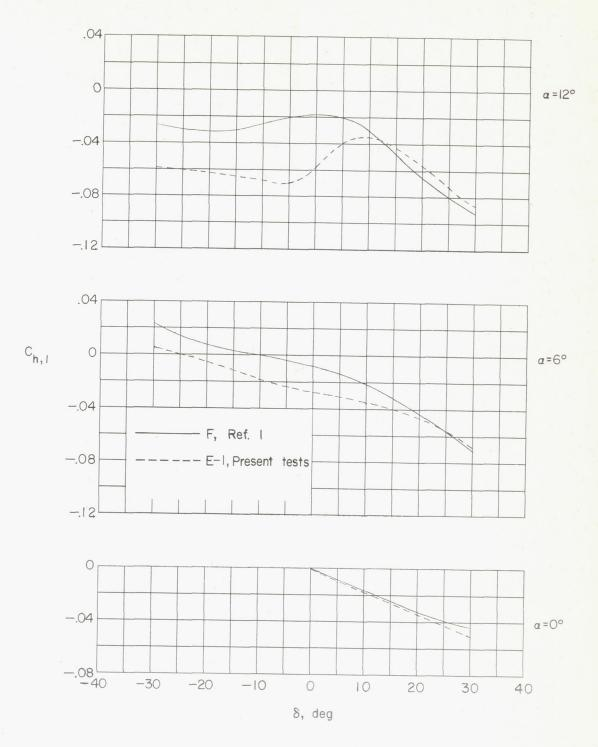
(a) Incremental hinge-moment-slope parameters due to tabs.

Figure 20.- Hinge-moment balancing effectiveness for tabs on configuration E. M = 1.61.



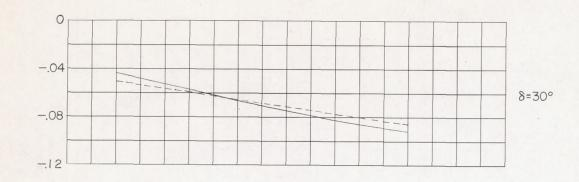
(b) Tab-to-control deflection required for  $(C_{h,1})_{\delta} = 0$ .

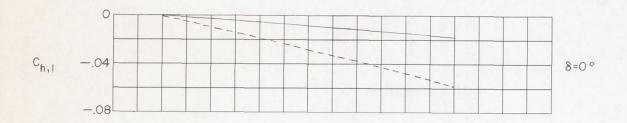
Figure 20.- Concluded.

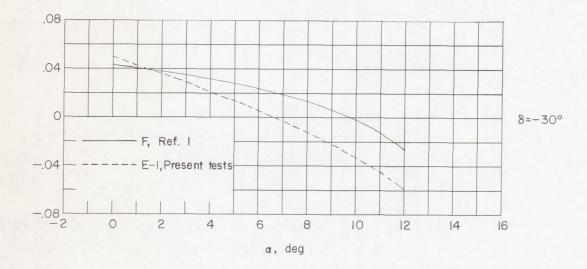


(a) Variation with  $\delta$ .

Figure 21.- Comparison of variations of hinge-moment coefficient of control with control deflection and angle of attack for configurations E-1 and F. M = 1.61.

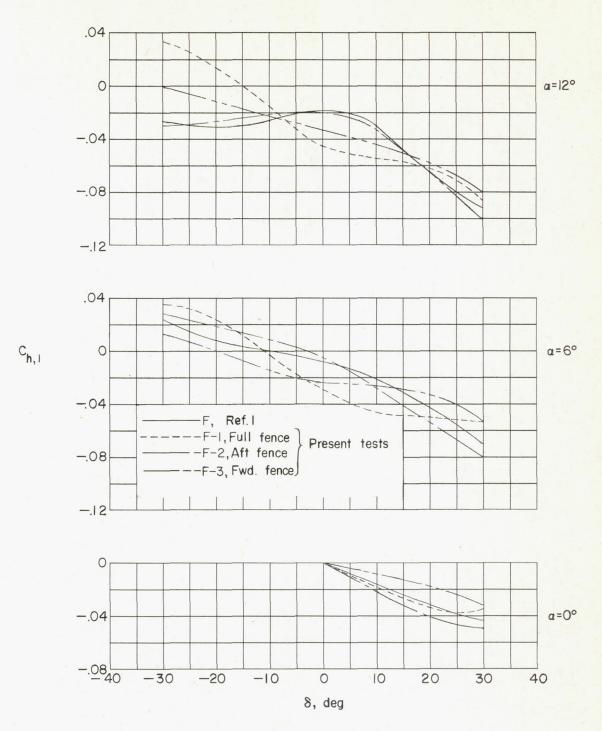






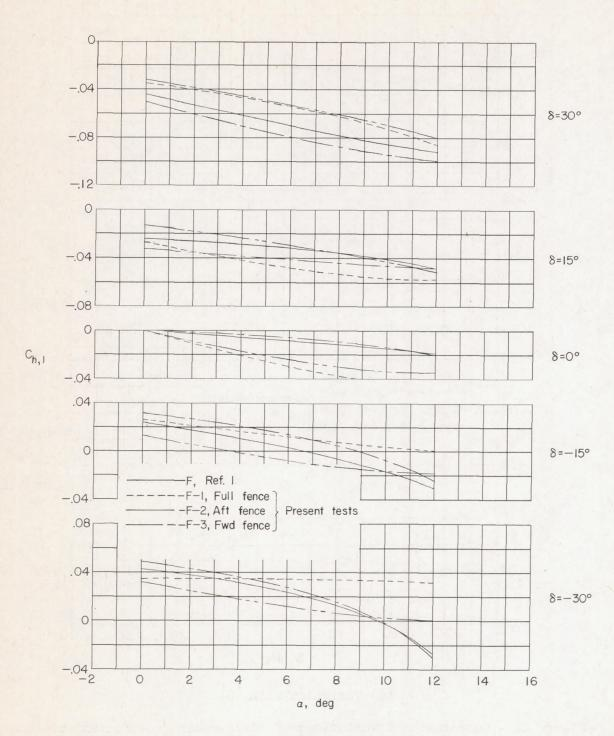
(b) Variation with  $\alpha$ .

Figure 21.- Concluded.

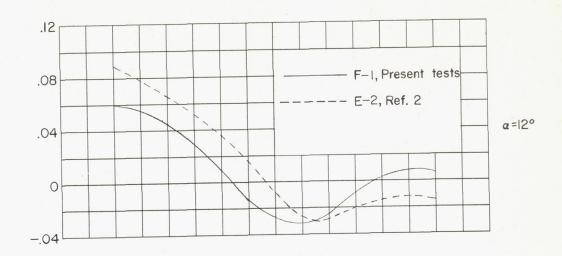


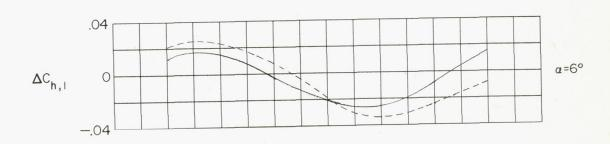
(a) Variation with  $\delta$ .

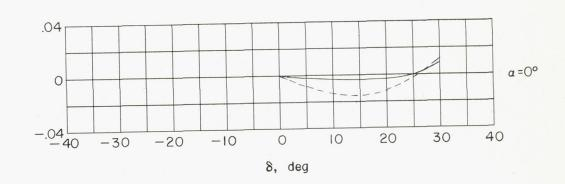
Figure 22.- Comparison of variations of hinge-moment coefficient of control with control deflection and angle of attack for fence configurations with those for configuration F. M = 1.61.



(b) Variation with  $\alpha$ . Figure 22.- Concluded.

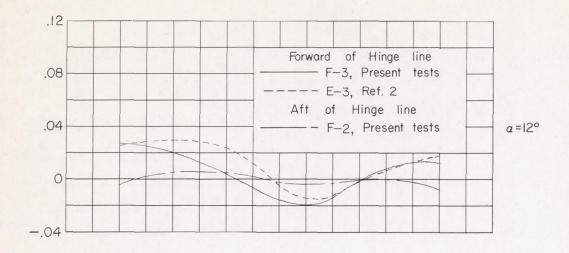


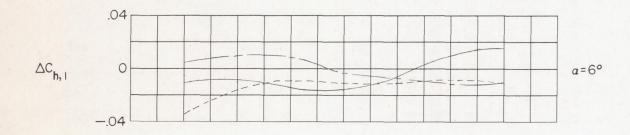


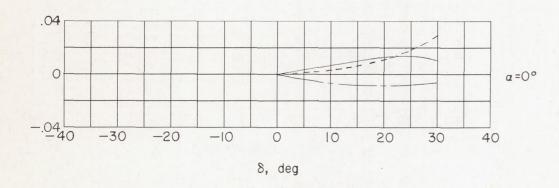


## (a) Full-chord fences.

Figure 23.- Comparison of incremental hinge-moment coefficients for fence configurations of present tests with those from reference 2. M=1.61.

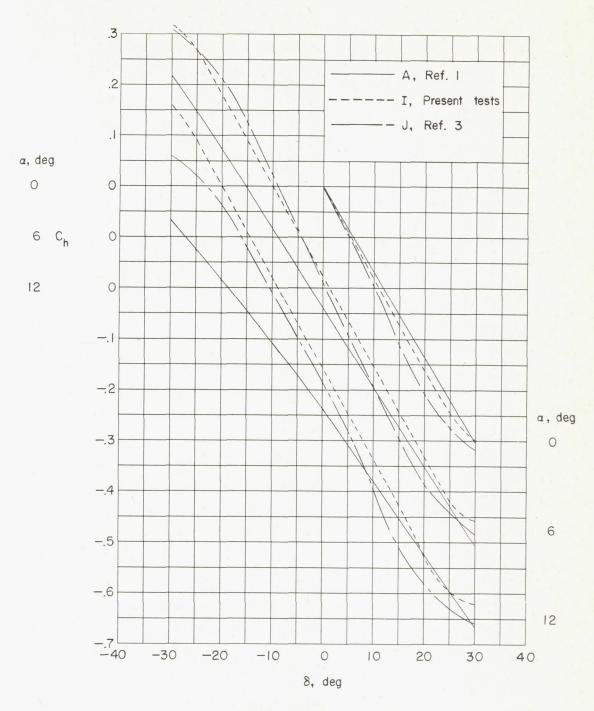






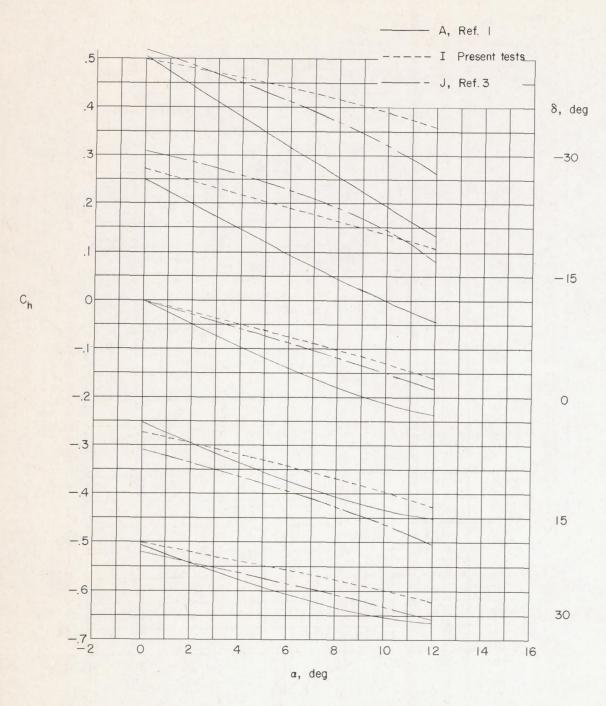
(b) Partial-chord fences.

Figure 23.- Concluded.



(a) Variation with  $\delta$ .

Figure 24.- Comparison of hinge-moment-coefficient variation of control with control deflection and angle of attack for three trailing-edge controls. M = 1.61.



(b) Variation with  $\alpha$ . Figure 24.- Concluded.

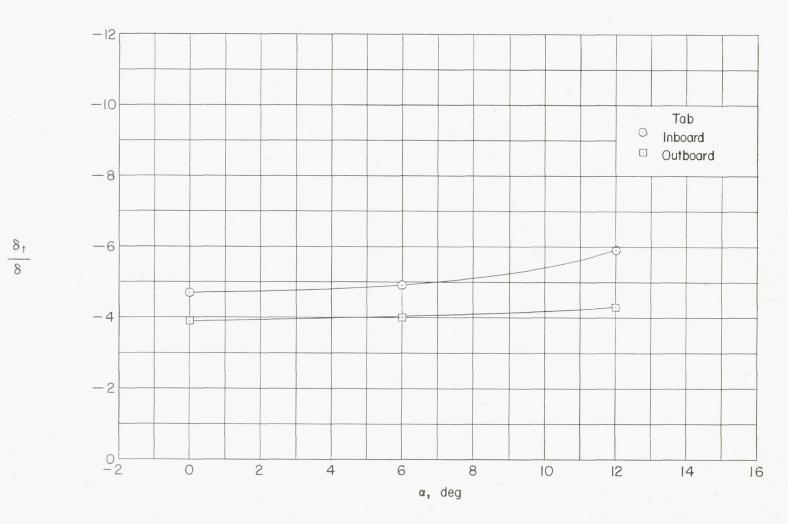
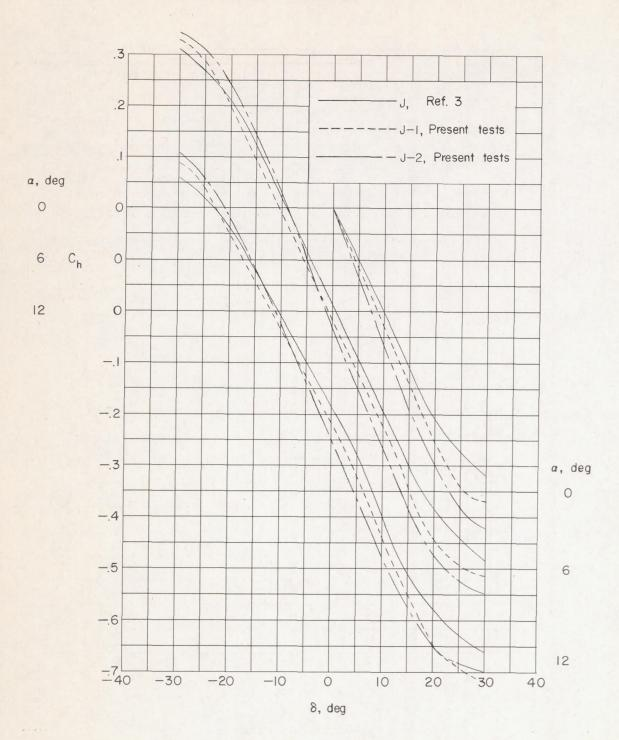
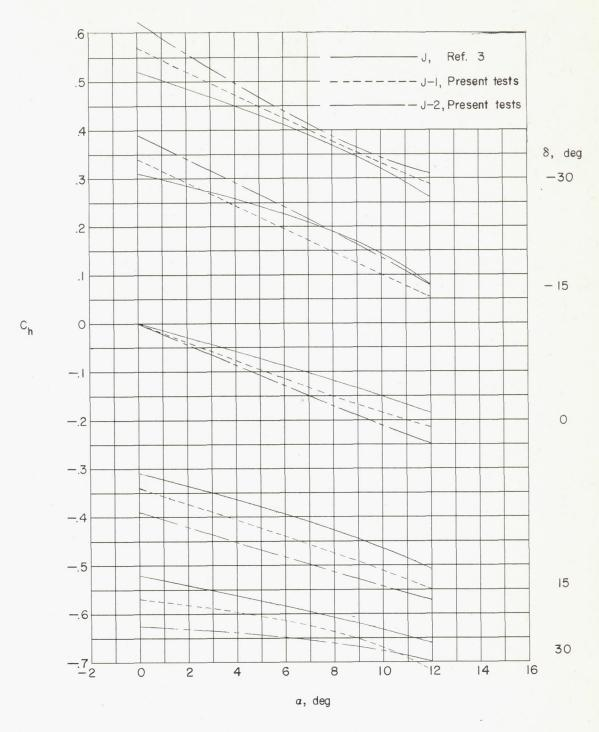


Figure 25.- Ratio of tab deflection to control deflection required for the attached tabs on configuration J to produce  $(C_h)_{\delta} = 0$ .

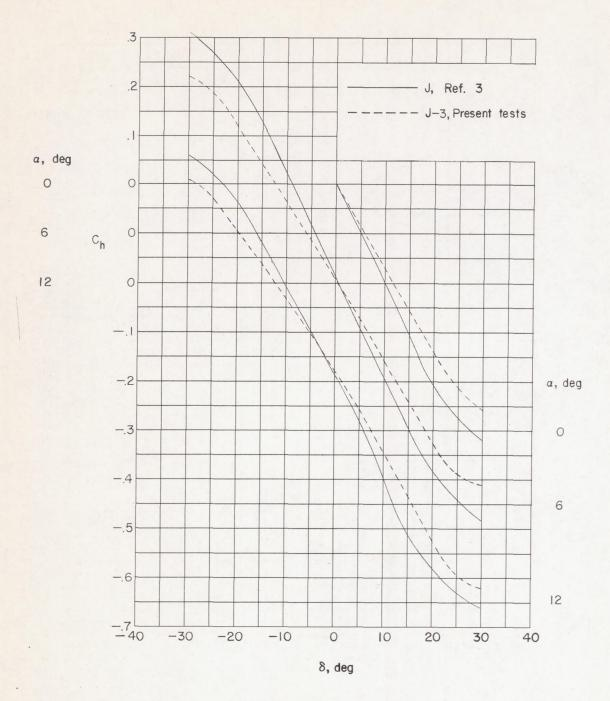


(a) Variation with  $\delta$ .

Figure 26.- Effect of trailing-edge thickness of control on variation of hinge-moment coefficient of control with control deflection and angle of attack. M = 1.61.

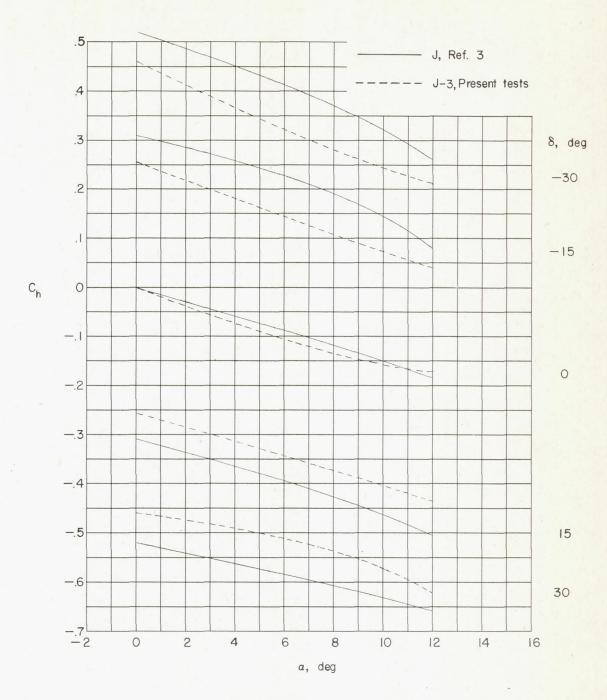


(b) Variation with  $\alpha$ . Figure 26.- Concluded.



(a) Variation with  $\delta$ .

Figure 27.- Effect of paddle balances on variation of hinge-moment coefficient of control with control deflection and angle of attack for full-span trailing-edge control. M = 1.61.



(b) Variation with  $\alpha$ .

Figure 27.- Concluded.